

This is the accepted manuscript made available via CHORUS. The article has been published as:

Heat conduction in deformable Frenkel-Kontorova lattices: Thermal conductivity and negative differential thermal resistance

Bao-quan Ai and Bambi Hu

Phys. Rev. E **83**, 011131 — Published 31 January 2011

DOI: [10.1103/PhysRevE.83.011131](https://doi.org/10.1103/PhysRevE.83.011131)

Heat conduction in deformable Frenkel-Kontorova lattices: thermal conductivity and negative differential thermal resistance

Bao-quan Ai^{1,2} and Bambi Hu^{2,3}

¹ *Laboratory of Quantum Information Technology, ICMP and SPTE,
South China Normal University, Guangzhou, China.*

² *Department of Physics, Centre for Nonlinear Studies,
and the Beijing-Hong Kong-Singapore Joint Centre
for Nonlinear and Complex Systems (Hong Kong),*

Hong Kong Baptist University, Kowloon Tong, Hong Kong, China

³ *Department of Physics, University of Houston, Houston, Texas 77204-5005, USA*

Abstract

Heat conduction through the Frenkel-Kontorova (FK) lattices is numerically investigated in the presence of a deformable substrate potential. It is found that the deformation of the substrate potential has a strong influence on heat conduction. The thermal conductivity as a function of the shape parameter is nonmonotonic. The deformation can enhance thermal conductivity greatly and there exists an optimal deformable value at which thermal conductivity takes its maximum. Remarkably, we also find that the deformation can facilitate the appearance of the negative differential thermal resistance (NDTR).

PACS numbers: 05.70.Ln, 44.10.+i, 05.60.-k

Keywords: Deformable potential, Frenkel-Kontorova lattices, heat conductivity, negative differential thermal resistance

I. INTRODUCTION

Heat conduction in low dimensional lattices is a well known classical problem related to the microscopic foundation of Fourier's law [1, 2]. The theoretical studies have not only enriched our understanding of the microscopic physical mechanism of heat conduction, but also suggested some useful thermal devices such as rectifiers or diodes[3], thermal transistors [4], thermal logic gates [5], and thermal memory [6]. People would like to know whether or not the Fourier law of heat conduction for bulk material is still valid in low dimensional systems. This is a fundamental question in nonequilibrium statistical mechanics. In general, the one-dimensional models can be classified into three categories [7]. The first one is integrable system such as the harmonic chain, in which no temperature gradient can be formed and thermal conductivity is divergent [8]. The second category includes some non-integrable systems such as the diatomic Toda chain [9], the Fermi-Pasta-Ulam (FPU) chain [10], Heisenberg spin chain[11], and so on. In these models, the temperature gradient can be formed but thermal conductivity is divergent at the thermodynamics limit. The third category contains the nonintegrable systems such as the ding-a-ling model [12], Lorentz gas model[13], ϕ^4 model[1], and FK model [14, 15]. In this category, thermal conductivity is finite and the Fourier's law is justified.

FK model was first proposed by Frenkel and Kontorova [14] in 1938 to study surface phenomena. Since then it has found application in wide variety of physics systems [15] such as adsorbed monolayers, Josephson junctions, and DNA denaturation. Despite its deceptively simple form, the model exhibits very rich and complex behaviors in heat conduction. For example, one can obtain the different frequency bands for different cases[3]: $\sqrt{\frac{V}{mL^2}} < \omega < \sqrt{\frac{V}{mL^2} + 4\frac{K}{m}}$ for low temperature limit, and $0 < \omega < 2\sqrt{\frac{K}{m}}$ for high temperature limit, where V is the height of the substrate potential, m is the mass of the particle, K is coupling constant, and L is the period of the on-site potential. The dependence of thermal conductivity on the temperature, the strength and the periodicity of the external potential, and the coupling constant is extensively studied [7, 15]. Shao and co-workers [16] studied the dependence of thermal conductivity κ on the strength of the interparticle potential K and the strength of the external potential V in the FK model and found the scaling form $\kappa \propto \frac{K^{3/2}}{V^2}$. Barik [17] studied the heat conduction of a two-dimensional FK lattice and found anomalous heat conduction. Zhong [18] studied a double-stranded system modeled by a

FK lattice and found that the interchain interaction has a positive effect on the thermal conductivity in the case of strong nonlinear potential, and has a negative effect on thermal conductivity in the case of weak nonlinear potential. In our previous work [19], we designed a thermal pumping by applying an external ac driving force at one boundary of FK lattice and found that the heat can be pumped from the low-temperature heat bath to the high temperature one by suitably adjusting the frequency of the ac driving force.

The study of heat conduction in low-dimensional systems also has practical implications. It has recently been found that nonlinear systems with structural asymmetry can exhibit thermal rectification, which has triggered model designs of various types of thermal devices such as thermal transistors [4], thermal logic gates [5], and thermal memory[6]. It is worth pointing out that most of these studies are relevant to heat conduction in the nonlinear response regime, where the counterintuitive phenomenon of negative differential thermal resistance (NDTR) may be observed and plays an important role in the operation of those devices. NDTR refers to the phenomenon where the resulting heat flux decreases as the applied temperature difference (or gradient) increases. It can be seen that a comprehensive understanding of the phenomenon of NDTR would be conducive to further developments in the designing and fabrication of thermal devices.

Most of studies are involved the regular potentials. However, in the real physical systems, the shape of the substrate potential can deviate from the standard (sinusoidal) one, and this may affect strongly the transport properties of the system [20]. The effects of the shape of the substrate potential on heat conduction is still lacking to date. In the present work, we study the heat conduction in deformable FK chains by using nonequilibrium molecular dynamics simulations. We emphasize on finding how the deformation of the potential affects thermal conductivity and NDTR.

II. MODEL AND METHODS

In this paper, we study heat conduction in FK chains with an asymmetric deformable potential. The Hamiltonian of the whole system is

$$H = \sum_{i=1}^N \frac{p_i^2}{2m} + \frac{1}{2}K(x_i - x_{i+1})^2 + U(x_i), \quad (1)$$

where p_i is the momentum of the i th particle, and x_i its displacement from equilibrium position. m is the mass of the particles, K is the spring constant and N is total number of the particles. In order to investigate the effects of the shape of the substrate potential on heat conduction, we use the following asymmetric deformable potential (shown in Fig. 1)[20]:

$$U(x) = \frac{V}{(2\pi)^2} \frac{(1-r^2)^2 [1 - \cos(2\pi x)]}{[1 + r^2 + 2r \cos(\pi x)]^2}, \quad (2)$$

where V is the height of the potential and r is the shape parameter. The potential reduces to the simply sinusoidal potential for $r = 0$ or $|r| \rightarrow \infty$. The degree of the deformation will increase when $|1 - r^2|$ decreases. The potential will disappear for $|r| = 1$. For convenience of discussion, we take the parameter range $0 < r < 1$, and in this parameter range, the degree of the deformation increases with r . For $0 < r < 1$, it is an asymmetric periodic one with a constant barrier height and two inequivalent successive wells with a flat and sharp bottom, respectively. This potential is considered as a natural way to describe lattice with diatomic basis or dual lattices by generalizing the standard model that assumes simple sinusoidal potential.

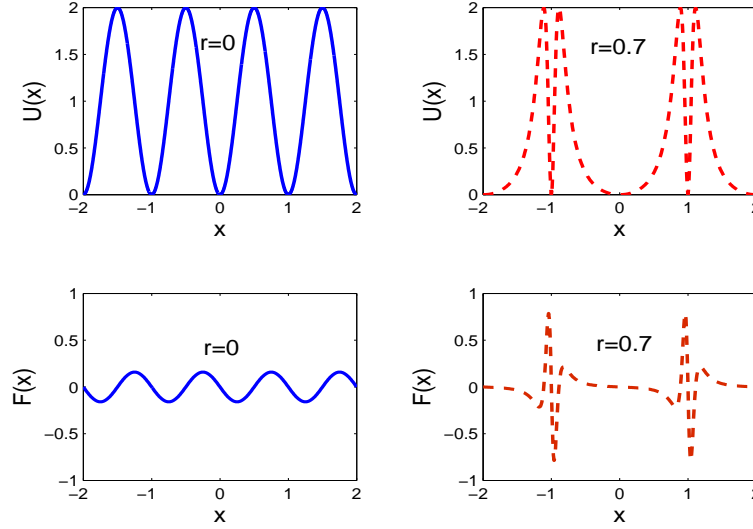


FIG. 1: (Color online) Asymmetric deformable potential for different values of the shape parameter $r = 0.0$ and 0.7 . The upper shows the potential $U(x)$ described in Eq. (2) and the bottom depicts its corresponding force $F(x) = -\frac{\partial U(x)}{\partial x}$.

As to obtain a stationary heat flux, the chain is connected two heat baths at temperature T_+ and T_- , respectively. Fixed boundary conditions are taken $x_0 = x_{N+1} = 0$. The equations of motion for the central particles ($i = 2, 3 \dots N - 1$) are

$$m\ddot{x}_i = -\frac{\partial U(x_i)}{\partial x_i} + K(x_{i+1} + x_{i-1} - 2x_i). \quad (3)$$

The equations of motion for $i = 1$ and $i = N$ particles are

$$m\ddot{x}_1 = -\frac{\partial U(x_1)}{\partial x_1} + K(x_2 - 2x_1) - \gamma\dot{x}_1 + \xi_-(t), \quad (4)$$

$$m\ddot{x}_N = -\frac{\partial U(x_N)}{\partial x_N} + K(x_{N-1} - 2x_N) - \gamma\dot{x}_N + \xi_+(t), \quad (5)$$

where γ is friction coefficient and the noise terms $\xi_{\pm}(t)$ satisfy the fluctuation dissipation relations $\langle \xi_-(t)\xi_-(t') \rangle = 2\gamma k_B T_- \delta(t - t')$, $\langle \xi_+(t)\xi_+(t') \rangle = 2\gamma k_B T_+ \delta(t - t')$, k_B being Boltzmann's constant. The dot stands for the derivative with respect to time t .

For simplicity we set the mass of the particles, the friction coefficient $m = \gamma = 1$. The local heat flux is defined by $J_i = k\langle \dot{x}_i(x_i - x_{i-1}) \rangle$ and the local temperature is defined as $T_i = \langle m\dot{x}_i^2 \rangle$. $\langle \dots \rangle$ denotes an ensemble average over time. After the system reaches a stationary state, J_i is independent of site position i , so that the flux can be denoted as J . Thermal conductivity is evaluated as

$$\kappa = \frac{NJ}{T_+ - T_-}. \quad (6)$$

Thermal conductivity represents an effective transport coefficient that includes both boundary and bulk resistances.

In our simulations, the equations of motion are integrated by using a second order Stochastic Runge-Kutta algorithm[21] with a small time step. Due to the deformation of the potential, the time step must be less than 10^{-4} for large values of r . The simulations are performed long enough to allow the system to reach a nonequilibrium steady state in which the local heat flux is a constant along the chain. To obtain a steady state, the total integration is typically 10^8 time units. We have checked that this is sufficient for the system to reach a steady state since the temperature profile in the central region is linear and the local heat flux is independent of the site.

We use Langevin heat baths instead of Nose-Hoover heat baths for the simulations because the use of Nose-Hoover heat baths might lead to unreliable results in the nonlinear response

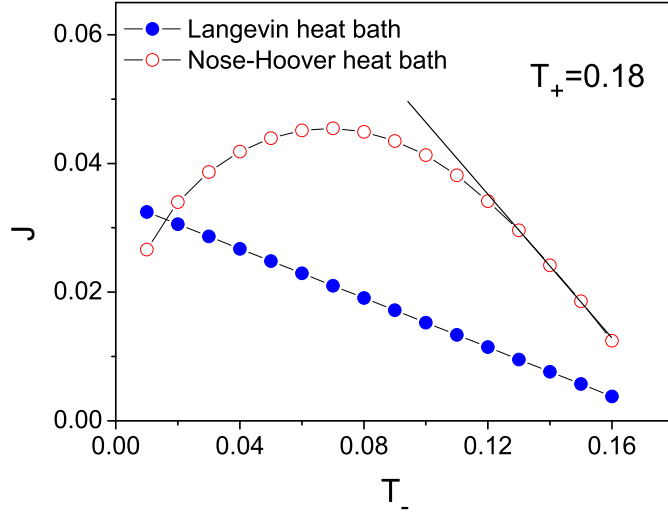


FIG. 2: (Color online) Heat flux J as function of T_- in pure harmonic model for different heat baths at $T_+ = 0.18$. For pure harmonic lattice, $U(x) = 0$ in Eq. (1) and $J \propto T_+ - T_-$. The other parameters are $N = 64$ and $K = 1.0$.

regime, particularly at very low or very high temperatures. The unreliable results are caused by either insufficient equilibration times or an artifact of using Nose-Hoover thermostats [22]. The pure harmonic lattice is a good model to check the validity of the thermostats. As we known, the heat flux in harmonic model increases linearly with the temperature difference, $J \propto T_+ - T_-$. However, from Fig. 2 we can see that the heat flux J as a function of temperature difference is nonmonotonic for Nose-Hoover heat baths, even NDTR occurs for large temperature difference. Obviously, it is not true. Therefore, we must be careful for using the Nose-Hoover heat baths. For Langevin heat baths, the heat flux increases linearly with temperature difference. The Langevin heat baths may be more reliable than Nose-Hoover heat baths.

III. NUMERICAL RESULTS AND DISCUSSION

Figure 3 shows thermal conductivity κ as a function of shape parameter r for different cases. From the figure we can find some interesting and surprising phenomena. The numerical results show that the deformation can enhance the thermal conductivity greatly. For

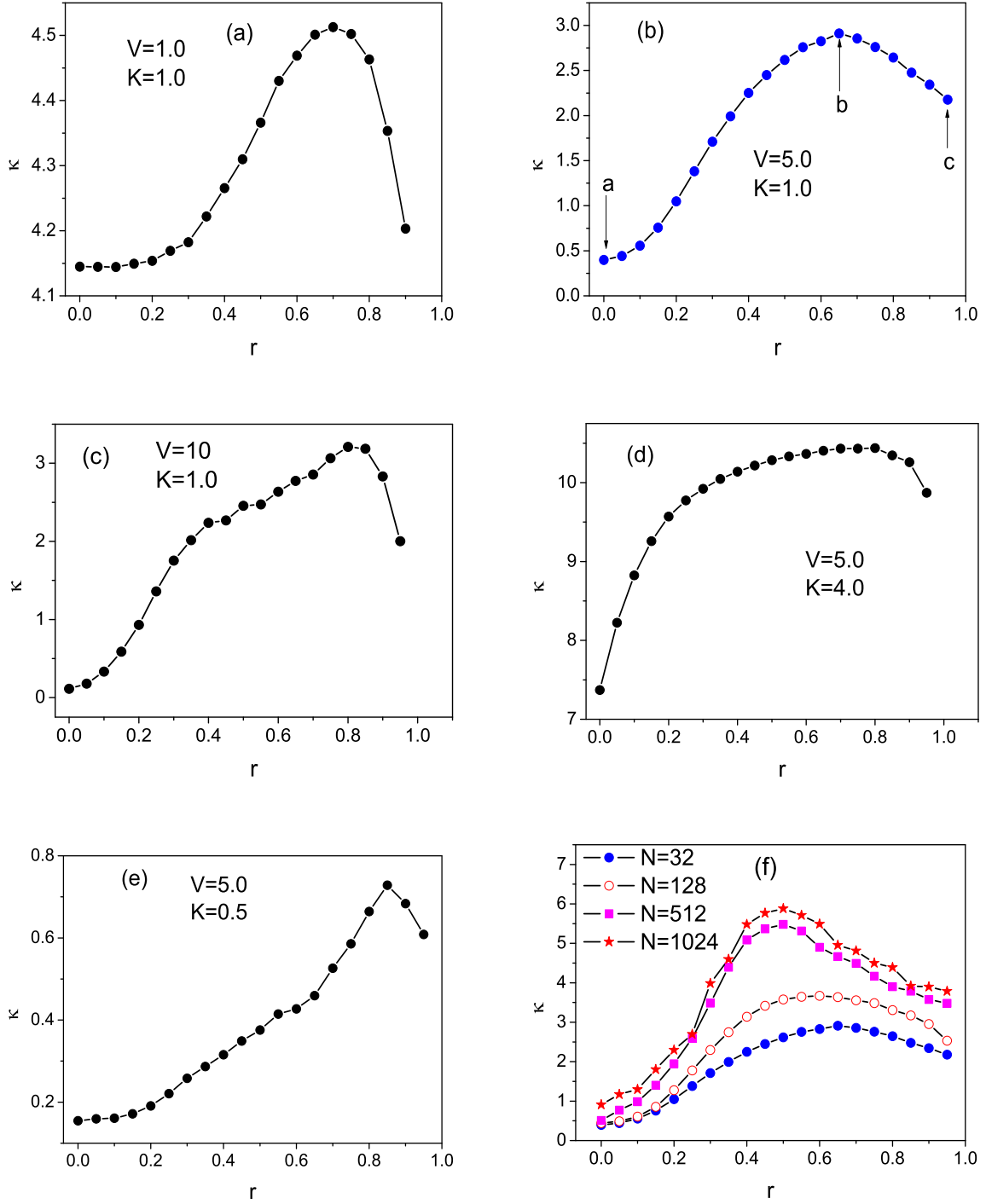


FIG. 3: (Color online) The dependence of thermal conductivity κ on the shape parameter r for different cases. (a) $V = 1.0$ and $K = 1.0$; (b) $V = 5.0$ and $K = 1.0$; (c) $V = 10.0$ and $K = 1.0$; (d) $V = 5.0$ and $K = 4.0$; (e) $V = 5.0$ and $K = 0.5$; (f) for different sizes $N = 32, 128, 512$, and 1024 at $V = 5.0$, $K = 1.0$. In (a)-(e) $N = 32$ and the other parameters are $T_+ = 0.2$ and $T_- = 0.1$.

example, for case of $V = 10$ and $K = 1.0$ (shown in Fig. 3 (c)), thermal conductivity can be increased by about 27 times ($\kappa = 0.113$ and 3.21 for $r = 0.0$ and 0.80 , respectively). The thermal conductivity κ increases at first and then decreases as the shape parameter r increases. There exists a value of r at which κ takes its maximum. Now we will give a physical interpret for the novel phenomenon. From Fig. 1, we can see that the deformable potential has two inequivalent successive wells with a flat and sharp bottom. When the particles stay in the flat well, the force acting the particle is very small, the heat is easy to be transferred from high temperature heat bath to the low one, resulting in a large thermal conductivity. Whereas the acting force is very large and the heat conductivity is small when the particles stay in the sharp well. When r increases from zero, the probability of the particles in the flat well is larger than that in the sharp one, the flat well dominated the heat conduction, so thermal conductivity increases. On further increasing r , the force acting the particles in the sharp well increases drastically, thermal conductivity is dominated by the sharp well, so thermal conductivity decreases. Therefore, there is a peak in the curves. Due to the universe finite size effect in low-dimensional systems, we consider more system sizes $N = 128, 512$, and 1024 , as shown in Fig. 3(f), thermal conductivity as a function of the shape parameter mentioned above is still invariant. Thermal conductivity increases to a saturation value when the system size increases since thermal conductivity of the FK model is finite in the thermodynamic limit. This indicates that these behaviors induced by the deformation of the potential are not the small-size effect. If the phenomenon disappears as the system size increases, the phenomenon is a small-size effect.

Figure 4 shows the temperature profiles for a , b , and c points shown in Fig. 3 (b). From the transition of the thermal transport mode we can also interpret the different thermal transport properties. Diffusive and ballistic regions are, respectively, corresponding to large and small temperature differences in the middle of the chain. The thermal conductivity can also be given by the Debye formula [1]

$$\kappa = \frac{c}{2\pi} \int_0^{2\pi} v(k)l(k)dk, \quad (7)$$

where c is the specific heat, $v(k)$ the velocity of the effective phonon, and $l(k)$ the mean-free path of the effective phonon. For ballistic region, both the velocity $v(k)$ and the mean-free path $l(k)$ are large, so the thermal conductivity is large. When the system goes into the diffusive region, both the velocity $v(k)$ and the mean-free path $l(k)$ decreases, therefore, the

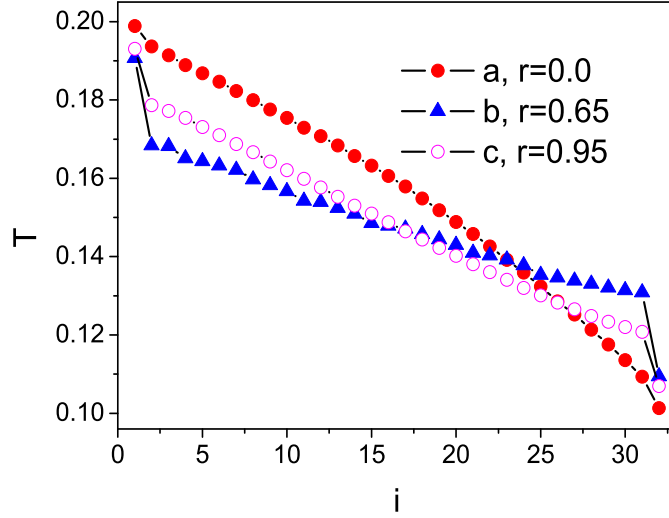


FIG. 4: (Color online) Temperature profiles for different values of r described in Fig. 3 (b).

thermal conductivity becomes small. It is easy to know that the flat well induces ballistic transport, whereas the sharp well contributes to diffusive transport. When the shape parameter r increases from $r = 0$, the temperature difference in the middle of the chain decreases (from a to b), which indicates that thermal transport mode exhibits a transition from the diffusive to the ballistic transport. Ballistic transport means less collision of phonon and then the thermal current will increase. On further increasing r , the temperature difference increases (from b to c), the system tends to diffusive transport and the thermal current decreases. The competition between the flat well (positive effect) and the sharp well (negative effect) determines thermal conductivity.

Figure 5 depicts the dependence of thermal conductivity on temperature for different values of r . Similar to the case of $r = 0$, thermal conductivity in deformable potential has a minimum at T_c . Thermal conductivity κ decreases monotonically with T_0 for $T_0 < T_c$ and increases monotonically with T_0 for $T_0 > T_c$. In FK model, there exist low and high temperature limits. For high temperature limit, $k_B T \gg \frac{V}{(2\pi)^2} \approx 0.13$, where the substrate potential is irrelevant, kinks do not play a role, and the FK chain behaves as a weakly interacting phonon gas. For low temperature limit, $k_B T \ll \frac{V}{(2\pi)^2}$, where the substrate potential is relevant and kinks play a role. For low temperatures, the deformation of the potential affects thermal conductivity drastically. However, the thermal conductivity becomes inde-

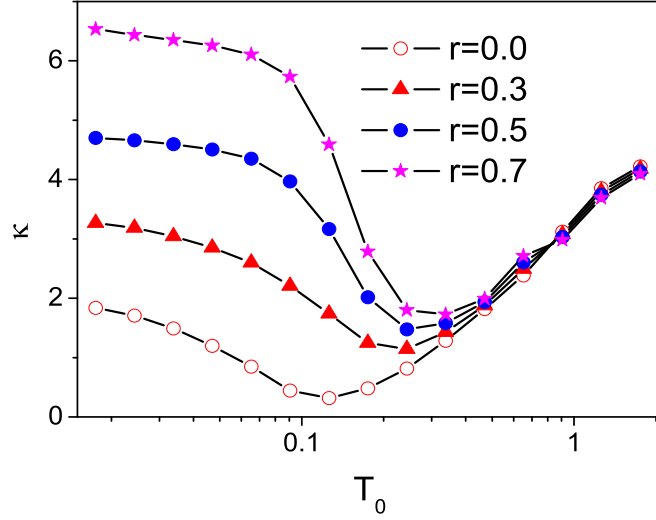


FIG. 5: (Color online) Temperature dependence of thermal conductivity κ for different values of $r = 0.0, 0.3, 0.5$, and 0.7 . Here $V = 5.0$, $K = 1.0$, $\Delta T = 0.02$, and $N = 32$. $T_0 = \frac{T_+ + T_-}{2}$, $\Delta T = T_+ - T_-$.

pendent of the deformation for very high temperatures. This is because the effect of the substrate potential disappears for high temperatures, each particle can jump freely between the minima of the substrate potential. The critical temperature T_c is dominated by the sharp well of the potential. The maximal force from the deformable potential is larger than that from the standard potential. The maximal force from the substrate potential increases with r . It needs higher temperature for all particles jumping freely between the two wells. Therefore, the critical temperature T_c shifts to the high temperatures on increasing r .

Now, we return to the phenomenon of NDTR, which refers to the phenomenon where the resulting heat flux decreases as the applied temperature difference(or gradient) increases. Figure 6 (a) shows the total heat flux NJ as a function of T_+ for regular ($r = 0.0$) and deformable ($r = 0.3, 0.5, 0.7$) FK chain, respectively, at $V = 5.0$, $K = 0.5$, $T_- = 0.01$, and $N = 32$. In our previous work [23], for regular FK chain, NDTR can occur for very low temperature $T_- = 0.001$. However, for $T_- = 0.01$, NJ increases with T_+ monotonically and no NDTR occurs. Interestingly, on increasing the shape parameter r , the system enters a nonlinear response regime where NDTR occurs. Therefore, the deformation of the potential

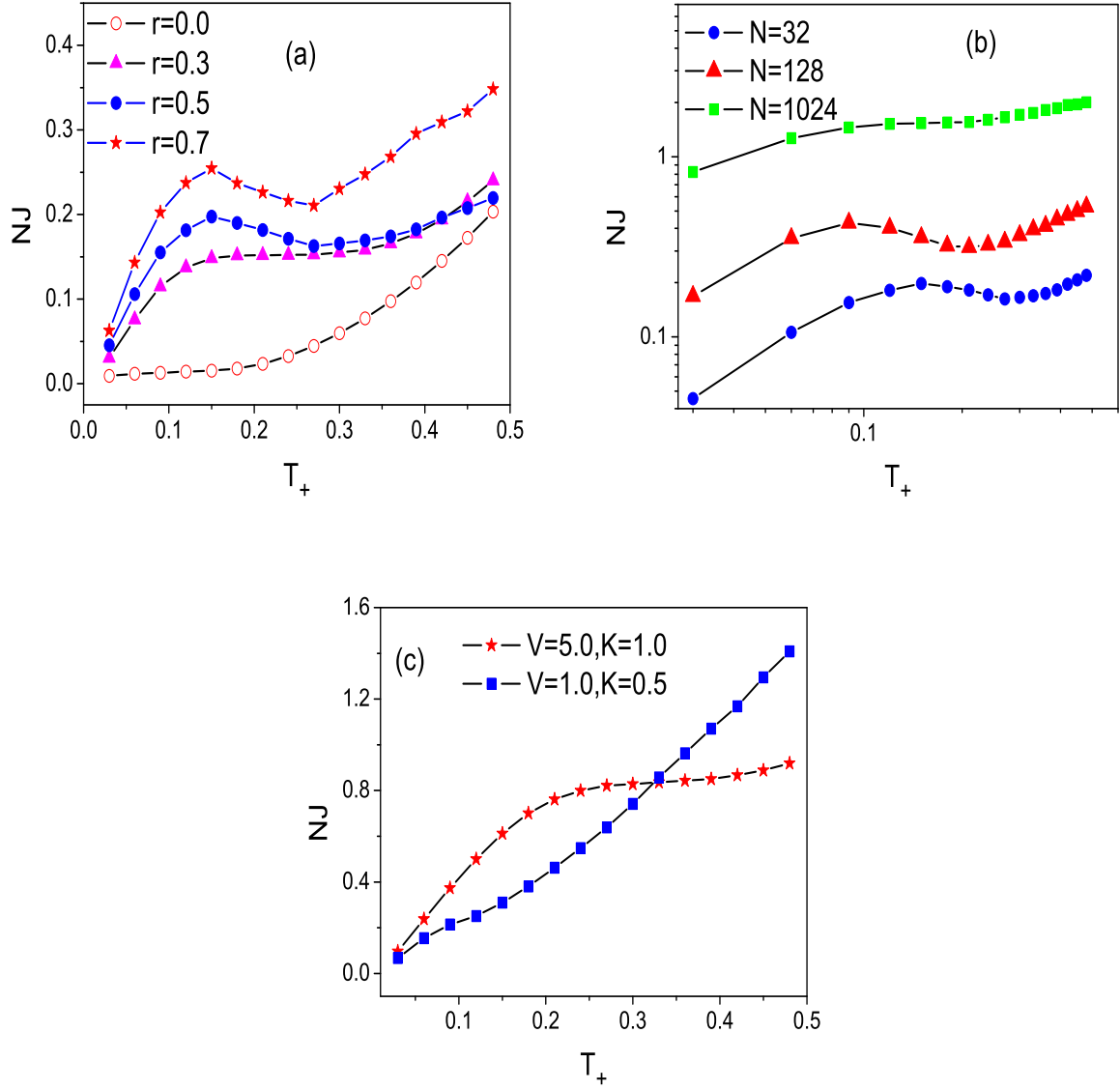


FIG. 6: (Color online) Total heat flux J as a function of T_+ for fixing $T_- = 0.01$. (a) For different values of r at $V = 5.0$, $K = 0.5$, and $N = 32$; (b) size effects on NDTR at $V = 5.0$, $K = 0.5$, and $r = 0.5$; (c) for different cases of $(V = 5.0, K = 1.0)$ and $(V = 1.0, K = 0.5)$ at $N = 32$ and $r = 0.5$.

can facilitate the appearance of NDTR. Figure 6 (b) shows the size effects on NDTR. The numerical simulations show the exhibition of NDTR for a system size of $N = 32$ and 128 but not for the case of $N = 1024$. This indicates that the regime of NDTR becomes smaller as the system size increases, and eventually vanishes in the thermodynamic limit. From Fig. 6

(c), we can see that the NDTR will disappear for decreasing V or increasing K . It becomes easier for the particles to overcome the on-site potential via their thermal energy when V decreases or K increases. Therefore, the system is approaching the harmonic limit where NDTR cannot occur. In general, it was found that NDTR may occur if there is nonlinearity in the on-site potential of the lattice model. However, in a deformable on-site potential, NDTR will occur in the larger range of the parameters.

As we know, thermal boundary resistance is more important in small-size systems. From the above results, we can find that NDTR also occur in small-size systems. Therefore, one can speculate that NDTR may be the result of some kind of boundary mechanisms. Figure 7 shows how the total heat flux NJ and the boundary temperature jump [24] $\delta T \equiv T(N) - T_-$ vary with T_+ . From the figure, we can see that total heat flux NJ exhibits the same relation with the boundary temperature jump δT for different cases. Therefore, NDTR may be caused by some boundary effects, for example, the phonon-boundary scattering or thermal boundary resistance. However, the general physical mechanism of NDTR for both two segment asymmetric FK chain [4] and the single chain described in this paper is not available. Especially, the necessary and sufficient conditions for NDTR are still lacking.

For convenience of numerical calculations, all physical quantities are dimensionless. However, it is necessary to give units of measurement for the potential experiments. First, it can give us very useful information about the corresponding true temperature to that one we used and enable us to gain some physical insights. The real temperature T_r is related to T through the relation [7, 25]

$$T_r = \frac{m\omega_0^2 L^2}{k_B} T, \quad (8)$$

where m is mass of the particle, $\omega_0 = \sqrt{K/m}$ is the oscillating frequency, L is the period of external potential, and k_B is the Boltzmann constant. For the typical values of atoms, we have

$$m \sim 10^{-26} - 10^{-27} kg, \quad k_B = 1.38 \times 10^{-23} JK^{-1}, \quad L \sim 10^{-10} m, \quad \omega_0 \sim 10^{13} sec^{-1}. \quad (9)$$

From Eqs. (8) and (9), we can find that $T_r \sim (10^2 - 10^3)T$, which means that the room temperature corresponds to the dimensionless temperature T about the order of $0.1 - 1.0$.

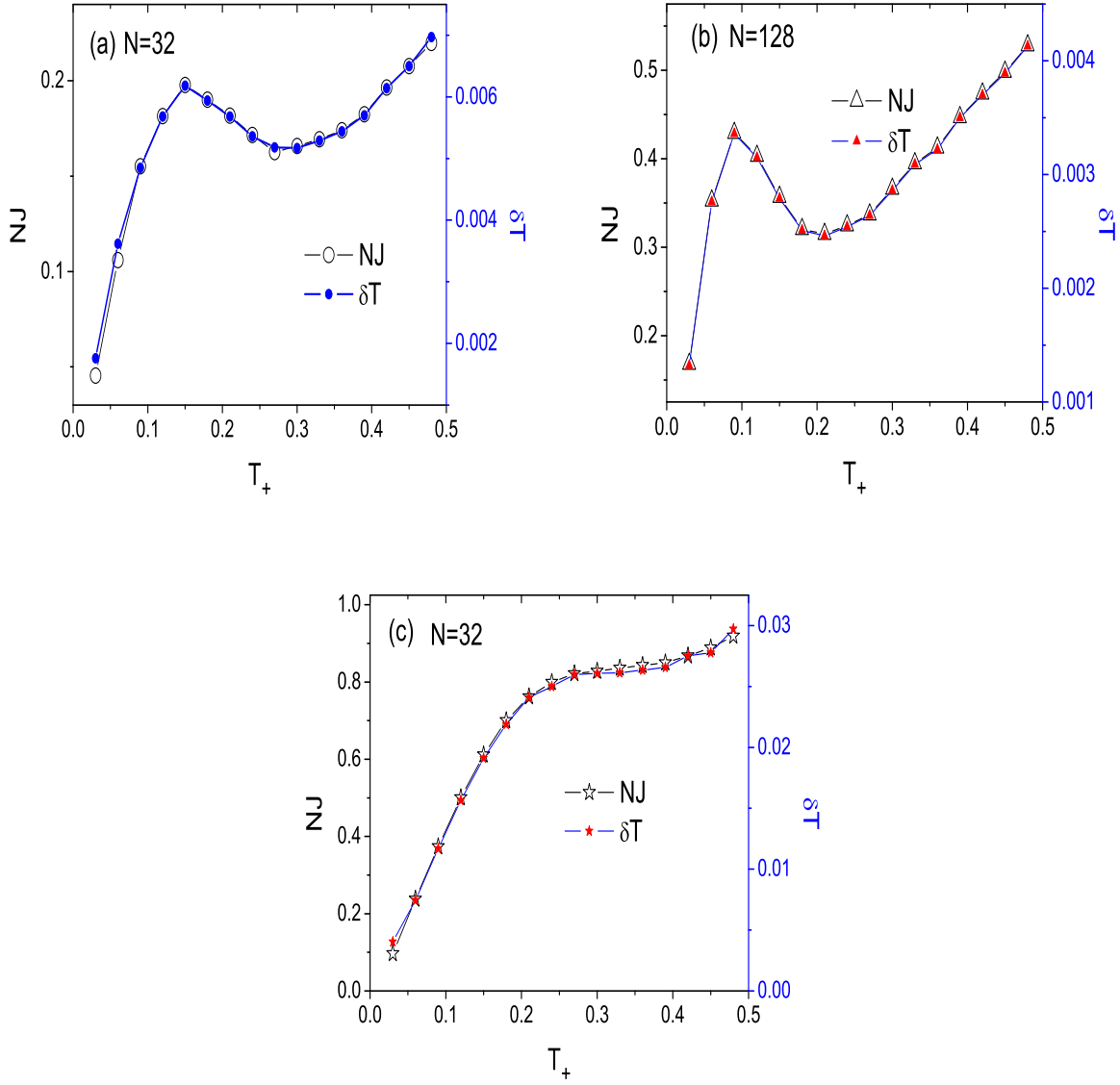


FIG. 7: (Color online) (a) Total heat flux NJ and the corresponding boundary temperature jump δT as a function of T_+ at $r = 0.5$. (a) $K = 0.5$ and $N = 32$; (b) $K = 0.5$ and $N = 128$; (c) $K = 1.0$ and $N = 32$. The other parameters are $V = 5.0$, $T_- = 0.01$, and $\delta T \equiv T(N) - T_-$.

IV. CONCLUDING REMARKS

In summary, heat conduction through the deformable FK lattices is extensively studied by using nonequilibrium molecular dynamics simulations. It is found that the deformation of the substrate potential induces the important effects on thermal conductivity and NDTR.

Thermal conductivity can be enhanced greatly by changing the shape parameter. Due to the competition between the sharp well and the flat well of the substrate potential, there exists an optimized value of r at which the thermal conductivity κ takes its maximal value. This behavior does not disappear as the system size varies. This means that the phenomenon is not a small-size effect, which is crucial for possible practical application as to control the heat flux. Thermal conductivity is drastically affected by the deformation for low temperatures, whereas the effect of the deformation will disappear for high temperatures. Interestingly, NDTR will appear when the shape parameter is increased, which may be observed and plays an important role in the operation of thermal devices [4–6]. It is easier to obtain the phenomenon of NDTR in the deformable FK lattices. The range of NDTR becomes smaller for increasing K or decreasing V . The phenomenon of NDTR will disappear in the thermodynamic limit ($N \rightarrow \infty$) and it is a small-size effect. We believe that the introduction of deformable FK model for heat conduction brings many interesting new features for physical applications, such as heat conduction in lattice with diatomic basis, dual lattices, or crystals with dislocations.

We would like to thank members of the Centre for Nonlinear Studies for useful discussions. This work was supported in part by Hong Kong Research Grants Council (RGC), the Hong Kong Baptist University Faculty Research Grant (FRG), National Natural Science Foundation of China (Grant No. 30600122), and GuangDong Provincial Natural Science Foundation (Grant No. 06025073).

-
- [1] S. Lepri, R. Livi, and A. Politi, Phys. Rep. 371, 1 (2003).
 - [2] A. Dhar, Advances in Physics 57,457(2008).
 - [3] B. Li, L. Wang, and G. Casati, Phys. Rev. Lett. 93, 184301 (2004).
 - [4] B. Li, L. Wang, and G. Casati, Appl. Phys. Lett. 88, 143501 (2006).
 - [5] L. Wang and B. Li, Phys. Rev. Lett. 99, 177208 (2007).
 - [6] L. Wang and B. Li, Phys. Rev. Lett. 101, 267203 (2008).
 - [7] B. Hu, B. Li, and H. Zhao, Phys. Rev. E 61, 3828 (2000); B. Hu, B. Li, and H. Zhao, Phys. Rev. E 57, 2992 (1998).
 - [8] Z. Rieder, J. L. Lebowitz, and E. Lieb, J. Math. Phys. 8, 1073 91967).

- [9] T. Hatano, Phys. Rev. E 59, R1 (1999).
- [10] S. Lepri, R. Livi, and A. Politi, Phys. Rev. Lett. 78, 1896 (1997); E. Fermi, J. Pasta, S. Ulam, in: E. Fermi (Ed.), Collected paper, University of Chicago Press, Chicago, 2, 78 (1976); L. Nicolin and D. Segal, Phys. Rev. E 81, 040102 (2010).
- [11] A. Dhar and D. Dhar, Phys. Rev. Lett. 82, 480 (1999).
- [12] G. Casati, J. Ford, F. Vivaldi, and W. M. Visscher, Phys. Rev. Lett. 52, 1861 (1984).
- [13] D. Alonso, R. Artuso, G. Casati, and I. Guarneri, Phys. Rev. Lett. 82, 1859 (1999).
- [14] Y. Frenkel and T. Kontorova, Zh. Eksp. Teor. Fiz. 8, 89 (1938).
- [15] B. Hu and L. Yang, Chaos 15, 015119 (2005).
- [16] Z. G. Shao, L. Yang, W. R. Zhong, D. H. He, and B. Hu, Phys. Rev. E 78, 061130 (2008).
- [17] D. Barik, Eur. Phys. J. B 56, 229 (2007).
- [18] W. R. Zhong, Phys. Rev. E 81, 061131 (2010).
- [19] B. Q. Ai, D. He, and B. Hu, Phys. Rev. E 81, 031124 (2010).
- [20] J. Tekic and B. Hu, Phys. Rev. E 81, 036604 (2010); M. Remoissenet and M. Peyrard, Phys. Rev. B 29, 3153 (1984).
- [21] R. L. Honeycutt, Phys. Rev. A 45, 600 (1992).
- [22] A. Dhar, Phys. Rev. Lett. 87, 069401 (2001).
- [23] D. He, B. Q. Ai, H. K. Chan, and B. Hu, Phys. Rev. E 81, 041131 (2010).
- [24] K. Aoki and D. Kusnezov, Phys. Rev. Lett. 86, 4029 (2001).
- [25] J. H. Lan and B. W. Li, Phys. Rev. B 74, 214305 (2006).